

Formation of supported bacterial lipid membrane mimics

Christoph Merz

Swiss Federal Institute of Technology Zurich (ETH Zürich), Wolfgang-Pauli-Strasse 10, CH-8093 Zurich, Switzerland

Wolfgang Knoll

Institute of Materials Research and Engineering, 3, Research Link, Singapore 117602, Singapore

Marcus Textor

Swiss Federal Institute of Technology Zurich (ETH Zürich), Wolfgang-Pauli-Strasse 10, CH-8093 Zurich, Switzerland

Erik Reimhult^{a)}

Swiss Federal Institute of Technology Zurich (ETH Zürich), Wolfgang-Pauli-Strasse 10, CH-8093 Zurich, Switzerland and Institute of Materials Research and Engineering, 3 Research Link, Singapore 117602, Singapore

(Received 26 November 2007; accepted 21 February 2008; published 30 April 2008)

In recent years, a large effort has been spent on advancing the understanding of how surface-supported membranes are formed through vesicle fusion. The aim is to find simple model systems for investigating biophysical and biochemical interactions between constituents of cell membranes and, for example, drugs and toxins altering membrane function. Designing and controlling the self-assembly of model membranes onto sensor substrates thus constitutes an important field of research, enabling applications in, e.g., drug screening, dynamic biointerfaces, artificial noses, and research on membrane-active antibiotics. The authors have developed and investigated the formation of strongly negatively charged supported lipid membranes which systematically mimic bacterial membrane composition on three important biosensor materials: SiO₂, TiO₂, and indium tin oxide. By tuning the electrostatic interaction through balancing the lipid vesicle charge with the ionic strength of Ca²⁺ as a fusion promoter, the authors have optimized the self-assembly and obtained new insights into the details of lipid vesicle-surface interaction. The results will be useful for future development and application of specialized lipid membrane surface coatings prepared from complex lipid compositions. The adsorption processes were characterized by a quartz crystal microbalance with dissipation monitoring, optical waveguide lightmode spectroscopy, and fluorescence recovery after photobleaching, which allowed the determination of formation also of nonplanar supported lipid membranes. © 2008 American Vacuum Society. [DOI: 10.1116/1.2896119]

I. INTRODUCTION

The various cell membranes are crucial structural and functional components of living cells. The outer cell membrane works as an efficient electrochemical delimiter of the cell and its surroundings, and simultaneously provides a scaffold for functional proteins controlling communication and transport with the outside environment.¹ Thus, the cell membranes contain a variety of components which are all associated with life-sustaining functions and the activity of the cell. With the complexity of real cell membranes and the organism they are surrounding, there has been a search for simpler model systems where their properties and the properties of their constituents as well as interaction with other molecules and influence of the environment can be investigated under controlled conditions. This typically entails combinations with surface sensitive techniques like surface plas-

mon resonance spectroscopy,^{2,3} waveguide spectroscopy,^{4,5} and a quartz crystal microbalance with dissipation monitoring.^{3,6,7}

One model system attracting considerable interest has been the supported lipid bilayer (SLB), formed as a planar lipid membrane at the interface of, e.g., a biosensor and thus functionalizing it with a lipid membrane exposing the distal leaflet to the bulk solution and the proximal leaflet toward the substrate.¹ SLBs are commonly prepared by a method pioneered by McConnell *et al.*,⁸ in which vesicles in bulk liquid are allowed to interact with a suitable surface, the latter inducing rupture and fusion of the vesicles to a coherent planar bilayer. The method produces—when successful—solvent-free fluid lipid bilayers spanning even macroscopic surface areas with few defects, which sets it apart from methods depending on solvent thinning or Langmuir-Blodgett transfer. This method of forming supported lipid bilayers has been investigated in detail by a number of groups for liposomes with a low complexity in terms of lipid composition. The formation of SLB from various phosphocholine (PC) lipid vesicles—sometimes mixed

^{a)}Author to whom correspondence should be addressed; electronic mail: erik.reimhult@mat.ethz.ch

with additional eukaryote lipids like phosphoserine (PS)—has been thoroughly investigated by, for example, the Boxer group,^{9–11} the Brisson group,^{7,12–17} the Decher group,^{18–20} the Kasemo group,^{3,6,21–24} and the Textor group.^{25,26} Silicon dioxide and titanium oxide have been mostly used for these studies, since the spontaneous decomposition of liposomes to SLB mainly occurs on these substrates under near-physiological conditions. Especially interesting results with implications for creating membranes that more closely mimic biological lipid compositions and often include a significant percentage of negatively charged lipids have been obtained by, e.g., the groups of Brisson, Textor, and others using fusogenic cations. They have shown that the presence of Ca^{2+} strongly promotes SLB formation in particular on TiO_2 while also leading to the asymmetric distribution of lipids between the two leaflets.^{13,14,16,25–29}

The main motivation for membrane research—including research using SLB—has been applications in drug screening, which has resulted in less attention to surface functionalization with membranes mimicking other organisms than eukaryote cells (cf. the references above). Thus, despite the number of publications in recent years on SLB formation and the in-depth knowledge generated, there are no similar investigations on how SLBs based on, e.g., bacterial lipids, can be self-assembled from liposomes' unfunctionalized biosensor substrates. Some previous attempts have been made toward creating SLB from liposomes including some relevant lipids for bacteria^{29–38} or even close to complete bacterial lipid mixtures.^{27,28,30,31,39,40} However, these studies have mostly used hydrophobic or polycationic polymers, which strongly promote liposome rupture in order to improve SLB yield, which resulted in incomplete and probably strongly pinned SLB, or else are low coverage preparations of SLB and vesicles on mica and glass substrates. There is also lacking an investigation of how these membranes are formed, and thus little knowledge for improving coverage and reproducibility of the SLB. Biosensors functionalized with lipid membranes mimicking bacteria would be a valuable tool given the increasing interest in devising new and understanding biologically derived antimicrobial agents.^{30,39–42} The mechanism for the antimicrobial activity of most known agents—whether synthetic or biologically derived—is at best sketchily understood, but a majority and increasing number of the evolutionary stable (i.e., not inducing resistant bacterial strains) antimicrobial molecules are believed to act against the bacterial membrane or receptors in that membrane.⁴² By functionalization of common biosensors for, e.g., waveguide spectroscopy or shear acoustic wave spectroscopy, it would be possible to learn in greater biophysical detail about the interaction between antimicrobial compounds and bacterial cell membranes. It would also be possible to devise quick screening protocols for their efficiency relative their effect on already existing eukaryote membrane mimics, without resorting to full-scale tests on cell.

We present an investigation of how to form solvent-free SLB on substrates of interest in biosensor research from liposomes which, to varying degrees of complexity, mimics

the cell membrane of *Escherichia coli* (*E. coli*) bacteria. It is demonstrated how the concentration of CaCl_2 can be varied to tune the vesicle-surface and vesicle-vesicle interaction to achieve vesicle adsorption, rupture, or other aggregated states at the interface. The process of liposome adsorption and SLB formation is shown to follow the same basic phases for the simpler bacterial model liposomes as observed previously for other compositions, but to be more sensitive to CaCl_2 concentration. The implications of these findings for the understanding of SLB formation induced by the presence of divalent cations is discussed in the context of previous work on PS-containing liposomes. A protocol is also described for forming SLB from liposomes of *E. coli* total lipid extract, having the full complexity of the lipid composition of the bacterial membrane. However, the *E. coli* SLB displayed an intriguing behavior revealed by application of several complementary techniques for investigating supported lipid layers. The analysis of the data indicates the membrane adopting a nonplanar geometry of potentially wider implication for the study of other complex lipid mixtures closely mimicking biological membranes.

II. MATERIALS AND METHODS

A. Materials

Ultrapure water (Millipore, France) was used for cleaning and buffer. HEPES [4(2-hydroxyethyl)piperazine-1-ethanesulfonic acid] and all salts were purchased from Fluka Chemie, Switzerland; sodium chloride and sodium dodecyl sulfate (SDS) were purchased from Sigma-Aldrich, Switzerland.

B. Substrates

Quartz crystal sensors (5 MHz, AT-cut, Q-Sense Sweden), were either purchased with 50 nm SiO_2 coating or coated with 12 nm TiO_2 or 50 nm indium tin oxide (ITO, In_2O_3 90%, SnO_2 10%) deposited by magnetron sputtering (in-house, Institute of Materials Research, Singapore). Optical waveguide light mode spectroscopy (OWLS) waveguides (MicroVacuum, Hungary) were coated with 12 nm of SiO_2 or TiO_2 by magnetron sputtering (Paul Scherrer Institute, Switzerland). SiO_2 -coated waveguides were annealed at 650 °C overnight to increase the stability of the coating before use. Cover glass slides were used as substrates for fluorescence recovery after photobleaching (FRAP) either as is or after coating with 12 nm TiO_2 by magnetron sputtering.

C. Cleaning

All substrates were cleaned before use in UV-ozone cleaner (Boekel UV Clean 135500, USA) for 30 min, which also results in a complete oxidation of the surface layer. After each measurement the sensors were cleaned *in situ* in the flow cells by flowing 2% SDS followed by thorough rinsing by copious amounts of ultrapure water and buffer at a flow rate of 250 $\mu\text{L}/\text{min}$. Substrates for FRAP and OWLS were cleaned with the same solutions but by exchange rinsing.

D. Sample solutions

All lipids were purchased from Avanti polar lipids (USA). The lipids used were 1-palmitoyl-2-oleoyl-*sn*-glycero-3-phosphocholine (POPC), 1-palmitoyl-2-oleoyl-*sn*-glycero-3-phosphoethanolamine (POPE), 1-palmitoyl-2-oleoyl-*sn*-glycero-3-[phospho-L-serine] (sodium salt) (POPS), 1-palmitoyl-2-[12-[(7-nitro-2-1,3-benzoxadiazol-4-yl)amino]dodecanoyl]-*sn*-glycero-3-phosphocholine (NBD-PC), *E. coli* total lipid extract (57.5 mol % PE, 15.1 mol % PG, 9.8 mol % cardiolipin, and 17.6 mol % other lipids). Five different kinds of liposomes in terms of lipid composition were prepared by bath sonication: POPC, POPC:POPS (8:2 w/w), POPC:POPG (2:1 w/w), POPE:POPG (2:1 w/w), and *E. coli* total lipid extract. First lipids stored in chloroform were mixed to the desired composition and dried into a thin film on the bottom of a round bottom flask continuously flushed with N₂ gas. The lipid film was resuspended in 10 mM HEPES buffer containing 150 mM NaCl to a concentration of 5 mg/ml. Aliquots of 1 ml were sonicated in a Pyrex test tube immersed at a point of high local intensity in a Branson 5210 ultrasonicator (Branson, USA). Typically the lipid solution turned completely clear in less than 10 min, and the total sonication time was 20 min per batch. Liposomes were characterized by light scattering using a Zetasizer 3000 Has (Malvern Inc., USA). The resulting liposomes are monodisperse with a relatively large size distribution: POPC 62 ± 22 nm, POPC:POPS 72 ± 26 nm, POPC:POPG 78 ± 31 nm, POPE:POPG 34 ± 12 nm, *E. coli* total lipid extract 77 ± 21 nm. In all experiments the stock solution was diluted to 50 μg/ml immediately before injection in the required buffer. Ten mM HEPES buffer with 150 mM NaCl was used for all experiments with different concentrations of CaCl₂ (0, 0.2, 1, 2, and 20 mM) or 2 mM EDTA added. Only the CaCl₂ concentration will be given in the rest of the text. Precinorm® U blood serum (Roche, Switzerland) consisting mostly of positively charged albumins at pH 7.4 was used for serum adsorption experiments.

III. MEASUREMENTS

All quartz crystal microbalance with dissipation monitoring (QCM-D) (Ref. 43) experiments were conducted using a Q-Sense E4 instrument (Q-Sense, Sweden) with four parallel measurement chambers. Thus, the same analyte was applied to the three different surfaces in the same experiment under equal conditions. All measurements were carried out at 50 μL/min buffer flow and 24 °C. Exceptions are the experiments on POPC:POPS liposomes on ITO, which were made on a Q-Sense D300 (Q-Sense, Sweden) by batch injection with a gravitationally driven flow. After stabilization of the baseline in buffer the solution was changed to the same buffer containing liposomes at 50 μg/ml concentration and the adsorption monitored for changes in resonant frequency, Δ*f*, and energy dissipation, Δ*D*, as a function of time using overtones 3 to 13 (~15 to ~65 MHz). Every experiment ended by rinsing with a pure buffer to remove weakly bound material. The mass can be approximately determined from Δ*f* using the Sauerbrey relation⁴⁴ for liposome and planar

supported lipid bilayers²³ using $\Delta m = -17.7 \Delta f / \nu$ ng/cm², where ν is the overtone number (all data are shown normalized to $\nu = 1$).

Optical waveguide light mode spectroscopy (OWLS) was performed on an OWLS 110 (MicroVacuum, Hungary).⁴ Samples were injected using syringes into a liquid cell at 24 °C and 50 μg/ml concentration after a stable baseline had been obtained through overnight incubation in the buffer. The OWLS measures changes in the effective refractive index, *n*, close to the interface simultaneously for two waveguide modes with different polarization. After resolving the refractive index and optical thickness of the adsorbed layer, de Feijter's formula⁴⁵ was used to calculate the mass of adsorbed lipids using $(dn/dc)_{\text{lipid}} = 0.18$. The value for *dn/dc* is not well defined in the literature and the value 0.18 cm³/g was chosen as an approximate median value found for planar lipid bilayers,^{3,46-48} where a higher value than for liposomes is expected due to alignment of the lipids in the evanescent field; the effective value could vary somewhat with lipid species.

Fluorescence recovery after photobleaching (FRAP) (Refs. 29, 49, and 50) was conducted with a confocal laser scanning microscope (CLSM, Zeiss LSM 510, Zeiss Germany). With all lipid mixtures, 2% NBD-PC (by weight) was used as a fluorescent marker. After liposome adsorption and possible SLB formation on a cover glass in an open cell, the liposome solution was exchanged for pure buffer. Rinsing was always done after an incubation time longer than needed to reach the asymptotically stable values in the QCM-D and OWLS experiments. A focused circular laser pulse (488 nm, 8.9 μm diameter, 100% intensity) was used to bleach a spot in the membrane. The fluidity of the membrane is measured by the rate and percentage recovery of fluorescence intensity of the bleached spot. The calculation of the diffusion coefficient was done based on the evaluation of Lopez *et al.*⁴⁹ and Axelrod *et al.*⁵⁰

The three techniques employed in this work are instructively complementary. The QCM-D measures water in addition to the lipid mass and is very sensitive to conformational differences like those between lipid vesicles and SLB on the surface. OWLS is, on the other hand, only sensitive to lipid molecules at the interface and, having the uncertainty in *dn/dc* described above in mind, one can quantify at least the relative amount of lipid material adsorbed at the interface. It is however difficult to distinguish between vesicle adsorption and SLB formation. Finally, while not very quantitative and supplying no information about kinetics, FRAP can be used to distinguish laterally connected SLB from nondiffusing vesicles and determine the fluidity through measuring the diffusion constant for species within the membrane. These techniques, when used together, allow even complex structures and phases to be resolved, which are easily overlooked or misinterpreted from a single set of data. For a further discussion of how this complementarity can be used for modeling see, e.g., Refs. 3, 47, and 51.

All three surface chemistries were screened under the different experimental conditions described above using

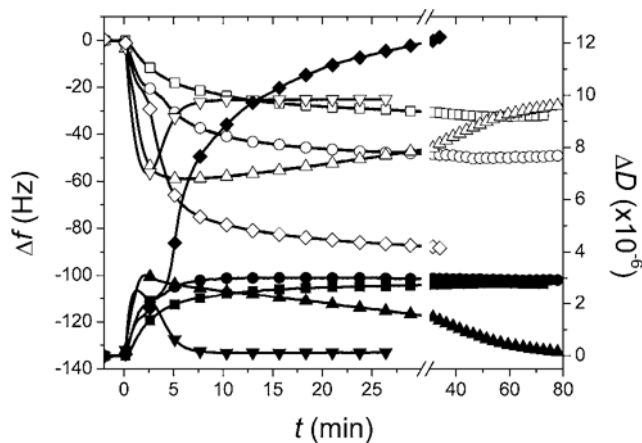


FIG. 1. QCM-D adsorption curves for POPC:POPG (2:1 w/w) liposomes as a function of CaCl_2 concentration in 150 mM NaCl, 10 mM HEPES buffer on SiO_2 . Open symbols show frequency shifts; filled symbols show dissipation shifts. 0 mM, squares; 0.2 mM, circles; 1 mM, upward-pointing triangle; 2 mM, downward-pointing triangles; 20 mM, diamonds. Trajectories for weak vesicle adsorption (0 and 0.2 mM), SLB formation (1 and 2 mM) and aggregation (20 mM) can be observed.

QCM-D and the adsorption trajectories classified as described in Sec. IV. The main focus was on finding conditions which produce SLB, so the most promising conditions and some controls were chosen for further characterization with CLSM and OWLS to measure lateral fluidity and approximate uptake of lipid mass. The criteria for determining whether a SLB was formed or not from QCM-D measurements were a final Δf close to 26 Hz and ΔD close to 0×10^{-6} when not stated otherwise, as have been demonstrated to be appropriate values corresponding to a SLB in various previous investigations.^{6,7,24,26} All measurements were repeated two times or more to check reproducibility.

IV. RESULTS

A. QCM-D trajectories for liposome surface interactions

Figure 1 shows examples of adsorption kinetics measured by QCM-D for the adsorption of POPC:POPG (2:1 w/w) on SiO_2 at different CaCl_2 concentrations. The different reproducible trajectories correspond to different outcomes of the adsorption process. For convenience we have grouped the trajectories into three main possible outcomes: (i) vesicle adsorption (cf. 0 and 0.2 mM CaCl_2 in Fig. 1); (ii) SLB formation (cf. 1 and 2 mM CaCl_2 in Fig. 1); and (iii) aggregation (cf. 20 mM CaCl_2 in Fig. 1). Of these three, the first two have well-known characteristic QCM-D kinetics established in earlier work.⁶ Vesicle adsorption yielding a monotonic increase in dissipation and a decrease in frequency with a high $\Delta D/\Delta f$ ratio can be distinguished from SLB formation with its typical three phase kinetics.^{3,6,52} After the initial vesicle adsorption, vesicle rupture starts to dominate over adsorption and a release of trapped water yields a net increase in f . Simultaneously, dissipation, originally high due to adsorbed soft vesicles, is decreased as the supported lipid bilayer is

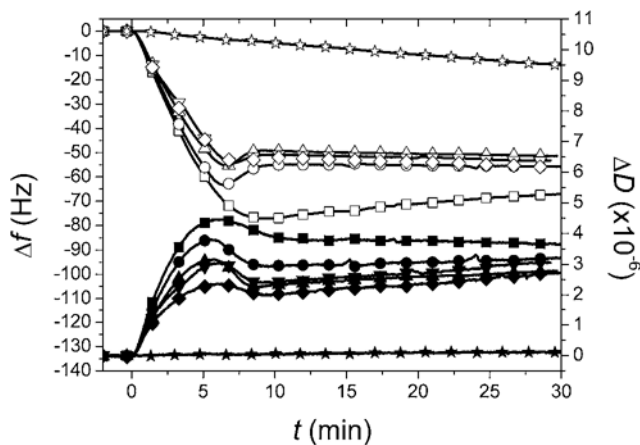


FIG. 2. QCM-D adsorption curves for *E. coli* total lipid extract liposomes adsorbing on TiO_2 at different CaCl_2 concentrations. Open symbols show frequency shifts; filled symbols show dissipation shifts. 2 mM EDTA, squares; 0 mM, circles; 0.2 mM, upward-pointing triangle; 1 mM, downward-pointing triangles; 2 mM, diamonds; 20 mM, stars.

formed, which is rigid to shear oscillations. After vesicle adsorption and rupture is completed the net change is $\Delta f = (-27) - (-24 \text{ Hz}) \sim 450 \text{ ng/cm}^2$ depending on lipid composition, and $\Delta D < 0.3 \times 10^{-6}$ depending on lipid composition, surface attraction, and number of defects.^{6,7,23} The aggregation behavior has previously not been characterized and will be further discussed below, but has previously been observed for lipid systems with high charge density and divalent cations.¹⁴ In terms of QCM-D response, aggregation was set to correspond to continuous high mass uptake at an increasing high $\Delta D/\Delta f$ ratio, which exceeds that observed for adsorption of a vesicle layer.

Two additional outcomes can be observed. The first is no adsorption at all, which has only rarely been observed for inorganic interfaces, but can be caused by strong charge repulsion.^{14,26} It is also possible to get a partial SLB formation, i.e., incomplete vesicle rupture, and end up with a stable mixture of vesicles and supported lipid bilayer islands on the surface. The former is recognized by QCM-D as no mass uptake, the latter typically as following the same kinetics as for SLB formation described above, but with an incomplete increase in f and decrease in D after the extreme points, yielding a remaining response of $\Delta f < -30 \text{ Hz}$ and $\Delta D > 1 \times 10^{-6}$ (cf. Fig. 2).

1. POPC:POPG and POPE:POPG liposome-substrate interaction

Tables I and II show the outcome of the screening for adsorption of POPC:POPG (2:1 w/w) and POPE:POPG (2:1 w/w), with the most optimal conditions for SLB formation highlighted. The results indicating SLB formation were further confirmed by OWLS measurements typically yielding a lipid mass close to 310 ng/cm^2 , yielding a corresponding area per lipid of $\sim 75 \text{ \AA}^2$, in the range of published area values for lipid bilayers.⁴⁸ Typical mass values obtained for vesicle adsorption were substantially higher and showed longer times for adsorption. FRAP was used as further veri-

TABLE I. Outcome of adsorption of POPC:POPG (2:1 w/w) liposomes to SiO₂, TiO₂, and ITO substrates at varying concentration of CaCl₂.

<i>c</i> (CaCl ₂) (mM)	SiO ₂	TiO ₂	ITO
0	Vesicles	No adsorption	...
0.2	Vesicles	Vesicles	Vesicles
1	SLB	Vesicles	Vesicles
2	SLB	Vesicles	Vesicles
20	Aggregation	SLB	Aggregation

fication that the standard interpretations of QCM-D and OWLS data could be applied also for bacterial mimic SLB. Typical recovered fractions of $\sim 90 \pm 10\%$ and diffusion coefficients on the order of $5 \times 10^{-9} \text{ cm}^2/\text{s}$ were obtained for SLBs, around 30% recovery for typical partial SLB formation and no recovery for vesicle adsorption. Although typically diffusion coefficients a factor of $\sim 2\text{--}4$ higher are found in the literature for phosphocholine SLBs on SiO₂/glass than measured for the bacterial mimic membranes,¹ we got identical diffusion coefficients $\sim 5 \times 10^{-9} \text{ cm}^2/\text{s}$ for POPC SLB on the SiO₂ substrates used in this study as for the bacterial membrane mimics.

2. E. coli total lipid extract liposome-substrate interaction

The results of QCM-D measurements for *E. coli* total extract liposome adsorption on TiO₂ at different concentration of CaCl₂ are shown in Fig. 2. A comparison of these data and kinetics to the typical case for SLB formation discussed in the beginning of Sec. IV seems to indicate that partial SLB formation (the local maximum and minimum in ΔD and Δf , respectively) initially occurs, followed by possible aggregation for *E. coli* total extract liposomes. Figure 3 shows data for *E. coli* total extract liposomes adsorbed on TiO₂ at 1 mM CaCl₂ concentration measured by QCM-D, OWLS, and FRAP, respectively. As can be observed, our preliminary analysis of the QCM-D data is contradictory to the other data sets. While the QCM-D indicates a continued mass increase and likely aggregation, the OWLS data show typical kinetics with a pronounced kink for SLB formation (cf. Refs. 3 and 51) and a continuous mass loss during the final phase. The FRAP recovery curves—one of which is displayed in Fig.

TABLE II. Outcome of adsorption of POPE:POPG (2:1 w/w) liposomes to SiO₂, TiO₂, and ITO substrates at varying concentration of CaCl₂.

<i>c</i> (CaCl ₂) (mM)	SiO ₂	TiO ₂	ITO
0	Vesicles	SLB	Vesicles
0.2	Partial SLB	SLB	Partial SLB
1	Partial SLB	SLB	Partial SLB
2	Aggregation	SLB	Aggregation
20	Very low and slow adsorption		

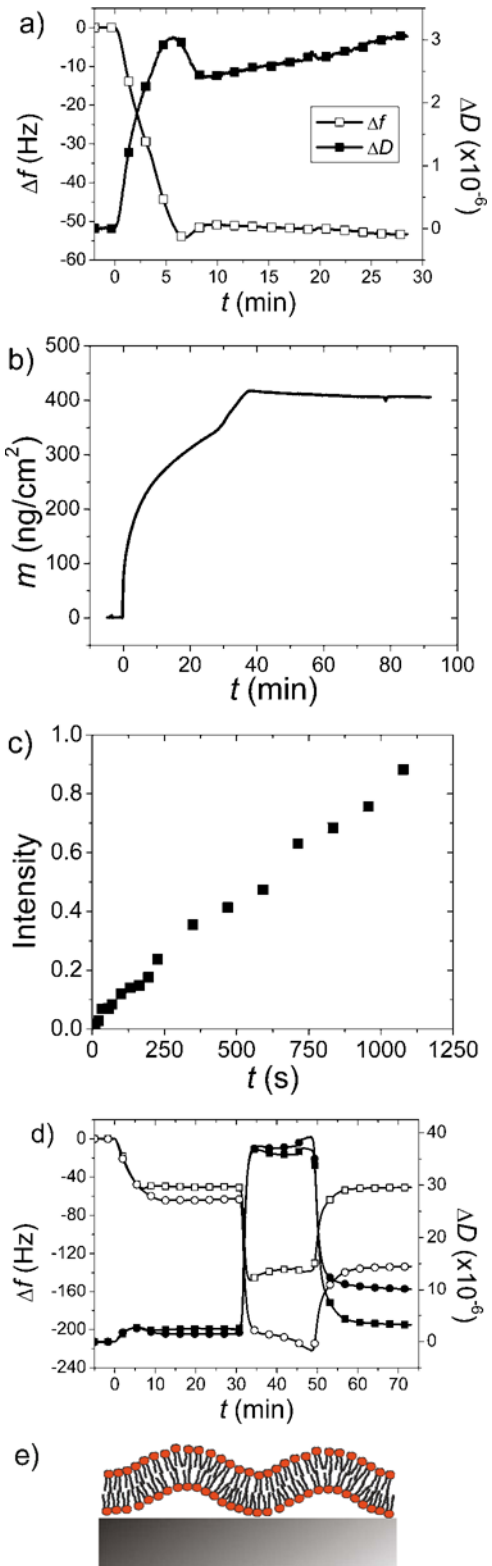


FIG. 3. Complementary measurements for *E. coli* total lipid extract liposomes adsorbing to TiO₂ in the presence of 1 mM CaCl₂. (a) QCM-D frequency (wet mass) and dissipation. (b) OWLS (dry) mass. (c) Fluorescence recovery after photobleaching of a spot in the adsorbed film. (d) Comparison of no adsorption of serum after addition to the adsorbed film on TiO₂ (Δf , open squares; ΔD filled squares) compared to significant adsorption for the partial SLB formed on SiO₂ (Δf , open circles; ΔD filled circles) under the same conditions. (e) Probable conformation of the adsorbed lipid film by comparison of the complementary measurements: a nonplanar SLB.

3(c)—shows that the lipid layer on the surface has a lateral fluidity allowing close to 100% recovery. The recovery is however much slower than usually observed for supported lipid bilayers and does not follow the expected profile for the bleaching geometry; thus, it cannot be accurately fitted to obtain a diffusion coefficient. Furthermore, a large variation—approximately a factor of 2—in recovery rate (comparing the almost linear slopes) was observed. The complementary results were similar to this for 0.2–2 mM CaCl₂ concentrations on TiO₂, where the QCM-D curves can be seen clustering close to each other.

V. DISCUSSION

In all the measurements a similar proportion (20–30 mol %) of anionic to zwitterionic lipids has been used, with the concentration of CaCl₂ varied in order to probe the liposome interaction with the different substrates under the influence of this known fusogen. Despite the similarities of the liposomes at first glance, strikingly different outcomes and kinetics could be observed, where the most complex of the lipid mixtures, *E. coli* total lipid extract, stands out.

A. *E. coli* total lipid extract SLB

QCM-D data for *E. coli* total extract liposomes seemed to indicate a partial SLB formation under most conditions on SiO₂ and TiO₂ and no conditions for a complete SLB formation. However, comparing the data sets in Fig. 3 for *E. coli* liposome adsorption on TiO₂ at 1 mM Ca²⁺ nominally showing partial SLB formation, it is clear that a conventional interpretation of the QCM-D data might be wrong. While after partial SLB formation QCM-D shows an increase in $\Delta D/\Delta f$, indicating a layer which couples more and more liquid, OWLS shows a decrease in the amount of lipid mass at the interface at the same time. Also, the FRAP measurement gives indisputable evidence of SLB on the surface, since SLB is the only laterally connected lipid structure that could yield a complete fluorescence recovery,⁵³ unless a complex network of interconnected liposomes is assumed. The latter is however not compatible with a decreasing OWLS mass when the QCM-D mass increases, since a growing network of interconnected liposomes would cause both QCM-D and OWLS mass to increase. Additionally, serum was added after completed adsorption which should not adsorb to SLB,⁵⁴ although it adsorbs strongly to the bare substrate in control experiments. Serum adsorption was not observed [Fig. 3(d)] after rinsing for the same systems where FRAP and OWLS indicated SLB formation and thus confirmed a complete SLB, but were observed in cases of only partial SLB formation to be more than 150 ng/cm². This observation is somewhat inconsistent with the quite high adsorption of serum on both SiO₂ and TiO₂ for POPC:POPS SLBs with similar anionic charge density observed by Rossetti *et al.*²⁵ The significantly lower serum adsorption on TiO₂ was interpreted as a result of most of the negatively charged PS head groups in the surface proximal leaflet, and the higher uptake on SiO₂ as binding of serum proteins to PS head groups through various mechanisms. It cannot be con-

TABLE III. Outcome of adsorption of *E. coli* total lipid extract liposomes to SiO₂, TiO₂, and ITO substrates at varying concentration of CaCl₂.

$c(\text{CaCl}_2)$ (mM EDTA)	SiO ₂	TiO ₂	ITO
2 mM EDTA	Partial SLB	Partial SLB	Vesicles
0	Partial SLB	Partial SLB	Vesicles/aggregation
0.2	Partial SLB	SLB	Vesicles/aggregation
1	Partial SLB	SLB	Vesicles/aggregation
2	Partial SLB	SLB	Vesicles/aggregation
20	Very low and slow adsorption		

cluded if the presented suppression of serum adsorption for, e.g., *E. coli* total lipid layers on TiO₂, but not on SiO₂, is due to a special binding of the serum to negatively charged lipids, e.g., in the presence of Ca²⁺, resulting in a stronger non-specific adsorption, or if there are other differences of importance in the preparations. One distinct difference is that *E. coli* total lipid has PG as the dominating negatively charged lipid and does not contain PS. Although, based on the results of Rossetti *et al.*, the serum binding to *E. coli* lipid layers on SiO₂ could be nonspecific adsorption to a SLB, the comparison of TiO₂ and SiO₂ results leads us to conclude the adsorption outcomes listed in Table III from the total set of data.

The complementary data sets can be reconciled if a non-planar SLB is considered. *E. coli* total lipid extract includes a multitude of lipid species which will prefer a curved membrane and could phase segregate to form a local high curvature. Partial phase segregation of lipid species could, e.g., be driven by local variations in ionic charge known to have a stronger attraction on certain lipids and could induce curvature.^{25,55} The local high concentration of cations at the substrate interface could in itself impose a higher curvature on one side of the membrane from variations in electrostatic screening across the membrane, as has been recently demonstrated.^{55,56} An increased water coupling of the QCM-D is to be expected if this causes *E. coli* SLB to increasingly undulate.¹⁴ Similarly, the average distance of the lipids within the evanescent field, which has a higher intensity and thus sensitivity closest to the interface, increases and the apparent sensed mass could decrease without an actual loss of lipid material from the SLB.^{51,57} A curved membrane at the interface also has a lower apparent refractive index to linearly *p*-polarized light in the OWLS evanescent field and thus an apparent lower mass loading when using this technique.⁴⁸ Finally, a nonplanar geometry with partially phase segregated lipids could explain the slower (but complete) fluorescence recovery and unusual diffusion profile. It has previously been described how, e.g., surface pinning of one lipid species can decrease the fluidity of another labeled lipid species, leading to altered diffusion profiles and recovery rates.^{13,25,58,59} A competing hypothesis of adsorbing additional layers of—possibly interconnected—liposomes on top of a first formed SLB which would fit, e.g., the QCM-D data and suppression of serum adsorption, does not agree with first and foremost the OWLS showing a decrease in

lipid mass rather than an increase, and is also difficult to reconcile with the lateral diffusion shown by FRAP.

B. Mechanism for SLB formation

The mechanism for formation of bacterial membrane SLB is likely similar to what was recently described by Rossetti *et al.* for DOPC:DOPS liposomes in the presence of Ca^{2+} .²⁶ This claim is supported by the higher instance of successful SLB formation with Ca^{2+} on TiO_2 than on SiO_2 . TiO_2 has a particularly strong interaction with Ca^{2+} ions and in the presence of Ca^{2+} the interface between TiO_2 and the buffer quickly gets saturated⁶⁰ and goes from a considerable negative zeta potential (-33 mV at pH 7.4) to more or less neutral.²⁶ This process does not occur on SiO_2 , where the slightly lower negative charge density than on TiO_2 stays approximately the same after Ca^{2+} addition.^{26,60–63} The presence of Ca^{2+} has been shown to promote the fusion of vesicles and SLB formation for a range of lipid species both on SiO_2 and TiO_2 ,^{7,14,16,17,25,26} but in particular for sufficiently high PS concentration (>20 mol %) negatively charged phosphoserine lipids on TiO_2 .²⁶ The latter is due to a strong complex formed between the PS head group and the Ca^{2+} at the TiO_2 interface.⁶⁰ Although this complexation might not occur for other anionic lipids such as, e.g., the PG head group present at a similar concentration in the bacterial membranes, the predominantly electrostatic interaction of the anionic head groups with the Ca^{2+} at the TiO_2 interface might cause an increased deformation of the liposome membrane once it has adsorbed to increase the probability of rupture. Previous investigations of bacterial liposomes have also indicated that the presence of Ca^{2+} as a fusogen increases the vesicle propensity to rupture at the interface.^{27,28,40} This is a likely interpretation of the facilitated formation of SLB on TiO_2 compared to SiO_2 under the same conditions. The objective in this study was to mimic *E. coli* lipid membrane composition and thus the concentration of anionic lipids was not systematically varied, but it is interesting to note that the concentration of those lipids is at or above the concentration threshold reported for DOPS lipids for SLB formation in the presence of Ca^{2+} on TiO_2 .²⁶ The presented results thus seem to indicate that the special complexation of PS- Ca^{2+} is not needed to increase the vesicle-surface interaction sufficiently for SLB formation on TiO_2 ; indeed, the local overcompensation of positive charge from Ca^{2+} at the interface can provide a sufficiently strong electrostatic attraction to anionic lipid head groups.

Another interesting note is that the choice of PE or PC as the bulk lipid has strong implications as well for whether SLB formation occurs. While POPC slightly favors SLB formation on SiO_2 , POPE strongly favors SLB formation on TiO_2 , as shown by comparing the results for POPC:POPG and POPE:POPG liposomes (Tables I and II). PC lipids have long been known to interact strongly with SiO_2 to form SLB,⁸ while POPE has not been much investigated yet in this respect. However, POPE has a conical shape factor with a negative intrinsic curvature, which will make it preferentially insert in the inner leaflet of a curved membrane.⁶⁴ The

smaller projected head group area to tail region of POPE has previously been proposed to facilitate the fusion and rupture of bulk liposomes, especially at modest molar ratios.⁶⁴ Rossetti *et al.* have suggested that the flip-flop of lipids between the leaflets when DOPS is enriched in the leaflet proximal to the substrate might in itself facilitate liposome rupture. With POPE creating a higher solvent accessible area in a planar membrane and with a driving force to enrich in the inner liposome leaflet, the mechanical stability of the membrane could be lower than for POPC and lead to a higher proportion of POPG already in the outer leaflet of the liposomes before adsorption, and a facilitated flip-flop of POPG upon adsorption. The pure effect on mechanical stability, however, does not seem to influence the trajectory significantly, given a comparison of the results on SiO_2 where POPE:POPG liposomes are more stable than POPC:POPG. The different results for POPE:POPG and POPC:POPG could also be due to differences in direct interaction between PE and PC head groups with the respective substrates. Given that SLB formation on TiO_2 occurs also at close to 0 mM Ca^{2+} for POPE:POPG liposomes and partial SLB formation for *E. coli* liposomes (containing 57.5 mol % PE) even when EDTA is added to remove any trace amounts of Ca^{2+} , this is a strong indication that POPE itself has a strong interaction with TiO_2 after the adsorption barrier has been passed, just like POPC has on SiO_2 . The relative deformation of liposomes on the surface before rupture can be estimated from the $\Delta D/\Delta f$ ratio, where a smaller ratio indicates a higher deformation.^{3,23,65} Furthermore, it is established that liposome deformation is related to the strength of the interaction with the substrate, and a higher deformation indicates a higher propensity to vesicle rupture and SLB formation.^{17,24,26,66,67} Thus, it is interesting in this context to note in Fig. 4 that differences in liposome deformation between TiO_2 and SiO_2 are small, especially for POPC:POPG and POPE:POPG liposomes. Rather, the main difference that is observed is just one of critical vesicle coverage before rupture occurs (cf. Refs. 21–23 and 68). For *E. coli* liposomes a slightly larger difference is observed. Thus, except for the case of *E. coli* liposomes, an initially stronger vesicle-surface attraction and deformation cannot explain the preferential SLB formation of one lipid mixture over the other.

For all substrates and liposomes, increasing the Ca^{2+} concentration to 20 mM resulted in a completely different adsorption kinetics. Typically, adsorption occurred at a much slower rate, although not as pronounced for POPC:POPG liposomes. Apparently the barrier to adsorption was increased and, additionally, some aggregation might have occurred already in the bulk, leading to a slower diffusion to the surface.

C. Liposome adsorption on ITO

So far, the difference between SiO_2 and TiO_2 has been discussed. A bit surprisingly, SLB formation was never found to occur on ITO under any of the screened conditions. Generally, liposomes only adsorbed very slowly with a high $\Delta D/\Delta f$ ratio, indicating a film of almost unperturbed lipo-

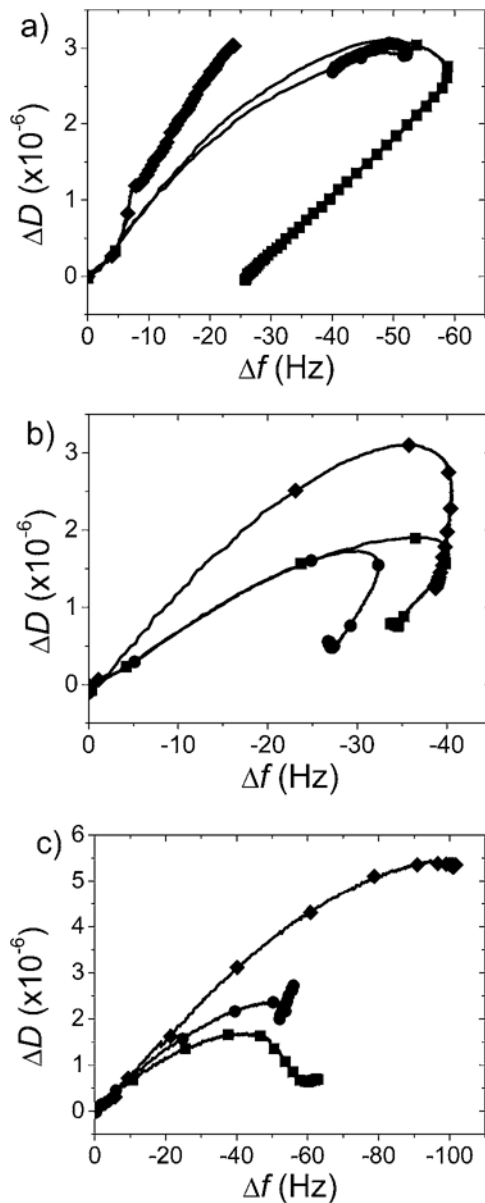


Fig. 4. Typical ΔD vs Δf plots for adsorption of the three different bacterial mimic liposomes on SiO_2 (squares), TiO_2 (circles), and ITO (diamonds). (a) POPC:POPG (2:1 w/w), 1 mM CaCl_2 . (b) POPE:POPG (2:1 w/w), 1 mM CaCl_2 . (c) *E. coli* total lipid extract, 2 mM CaCl_2 . Similar ratios of ΔD to Δf indicate similar deformation of liposomes on the surface. For *E. coli* liposomes a significant difference in $\Delta D/\Delta f$ is observed, while for POPC:POPG and POPE:POPG liposomes the initial slopes only show small variations between the different conditions.

somes or multilayers of liposomes adsorbed weakly at the interface. If Ca^{2+} concentration was increased to induce rupture, the typical result was aggregation occurring on the surface. This was rather unexpected since preliminary measurements using liposomes with similar negative charge, but a mixture of POPC and POPS as well as vesicles containing 100% POPC, could be made to fuse to ITO under some conditions (Fig. 5). While the formation of SLB from POPC:POPS (8:2 w/w) liposomes was highly reproducible, SLB formation for 100% POPC did not always occur, which indicates a high sensitivity for this process to minor varia-

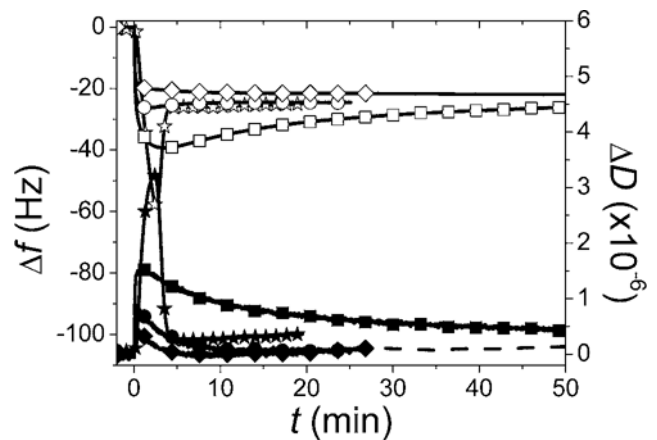


Fig. 5. QCM-D kinetics (open symbols show frequency shifts; filled symbols show dissipation shifts) of adsorption of POPC (0 mM CaCl_2 , stars) and POPC:POPS (8:2 w/w) liposomes (0 mM CaCl_2 , squares; 1 mM CaCl_2 , circles; 2 mM, diamonds) on ITO.

tions in properties of ITO coatings and/or experimental conditions beyond current control. Especially for the POPC:POPS liposomes, it was observed that the extremum points in both Δf and ΔD , which indicate the buildup of a critical coverage of vesicles on the surface before vesicle rupture and SLB formation starts,^{22,26,68} were very low. This is a strong indication that a significant rupture of single liposomes occurs directly upon adsorption, without the need for critical coverage as previously observed on, e.g., mica.¹⁷ Furthermore, correlating with this suppression of extremum values is a reduced total mass measured by the QCM-D for the SLB, which in itself signals an unusually strong interaction between the SLB and substrate, possibly leading to a complete removal of the ~ 1 nm water film between the SLB and the substrate⁶⁹ at 2 mM CaCl_2 , where the SLB mass is reduced by one fifth, although without additional verification it cannot be ruled out that there is an incomplete coverage of SLB giving rise to this response. Only a few cases of SLB formation on ITO have previously been demonstrated, but they have also required formation in solvent,^{38,70} on a polymer brush^{71,72} or by annealing of positively charged membranes.^{73,74} None has examined the detailed structure of the film, which could be compared to the results presented here indicating a closely adhering SLB on the ITO.

D. Partial SLB formation

Typically, SLB formed by liposome fusion contains a small number of defects occupied by liposomes, which in QCM-D data is revealed as a dissipation shift slightly higher than 0×10^{-6} and a less than full recovery in FRAP. These are however typical variations for SLB formation on macroscopic samples, and only conditions showing a remaining high percentage of the surface covered by liposomes should be classified as partial SLB. Partial SLB formation was primarily observed for *E. coli* total extract liposomes on SiO_2 , although it cannot be ruled out that vesicles not undergoing rupture are still remaining on the surface in some of the other

cases classified as SLB. Partial SLB formation occurs when the driving force for vesicle rupture is not strong enough to force rupture of all vesicles, or possibly when lipids on the surface are too strongly pinned to spread the rupture to liposomes on the entire surface.

E. Aggregation

The adsorption trajectory referred to as aggregation was observed mainly when the concentration of Ca^{2+} was increased. This could occur for a certain substrate after either vesicle adsorption had occurred at a lower Ca^{2+} concentration or after vesicle adsorption, and then at least partial SLB formation had been observed at higher Ca^{2+} concentration. If the resulting increase in coupled mass and dissipation resulted from the fusion of smaller vesicles into larger, the $\Delta D/\Delta f$ ratio (ΔD increasing rapidly for a small decrease in Δf , cf. the 20 mM Ca^{2+} curve in Fig. 1) would be lower.²³ Instead, the strongly increasing $\Delta D/\Delta f$ ratio, together with the increase in absolute frequency and dissipation shifts, strongly suggests an extended matrix of coupled vesicles adsorbed in multilayers. These could either be loosely associated with each other or form an interconnected network of hemifused liposomes. It could also be a sign of that a significant aggregation of liposomes occurs already in solution at these Ca^{2+} concentrations, as is known to occur for some lipid compositions, although to our knowledge not studied for the systems under investigation here. However, while the process is significantly slowed down after the removal of liposomes from the bulk solution, it still seems to occur. This behavior is similar to what has been observed and named restructuring for DOPC:DOPS vesicles in the presence of 2 mM Ca^{2+} ,¹⁴ although for those preparations the addition of 2 mM EDTA collapses the soft structure to something similar to a SLB. The mechanisms at work in that case and for the aggregation behavior of the bacterial membrane mimics presented here are probably closely related, despite the important differences in terms of reversibility and much faster formation and extension of the formed structures for bacterial mimics.

Interestingly, while aggregation obviously resulted in an extended film, the substrate obviously plays a role for whether aggregation occurs or not. It cannot be fully explained as the aggregation of negatively charged vesicles due to bridging by Ca^{2+} ions, since it is not observed under identical conditions on the different substrates and also did not seem to correlate with the overall liposome charge density of anionic lipid. These are strong indications that what is observed is a surface induced effect, which at most is modified but not dominated by, e.g., liposome aggregation in the bulk. It can also be observed that aggregation occurred at a lower Ca^{2+} concentration for POPE-rich liposomes, which in addition to being more bacteriallike than their POPC equivalent also should be more fusogenic due to the symmetry breaking shape of PE.⁶⁴ The formation of hemifused liposomes^{64,75} promoted by PE lipids and a particular surface deformation of the first layer of vesicles could be one hypothesis to explain these findings. Whatever the interaction, it is suffi-

ciently strong to make it impossible to remove the aggregated structure either by rinsing at high shear flow or by introducing EDTA buffer to remove the calcium, but studies on hemifused liposomes have shown them to be quite stable systems⁷⁵ Only further aggregation could be prevented this way. It thus seems plausible that, as suggested before, a conformational change occurs at open edges in the membrane.¹⁴ Possibly the more dissimilar shape factors of the lipids in the bacterial mimics aid faster formation and induce stronger curvature in an extended deformed membrane, which leads to such deformed conformations that even by removal of Ca^{2+} the kinetic barrier to go back to a more planar, fully connected SLB is too high for it to be observed.

F. Implications for SLB formation from complex mixture anionic liposomes

The mechanism for forming SLB from net anionic liposomes using Ca^{2+} as a mediator and facilitator appears, from the presented results, robust and not limited to a special strong interaction with PS head groups. As long as a sufficiently high mol-percentage of anionic lipids, tentatively >15–20% is present, SLB formation can be achieved in the presence of a low concentration of Ca^{2+} on TiO_2 , and under more restricted conditions on SiO_2 . However, a too high Ca^{2+} concentration, which from a few exploratory experiments could be as low as 2–5 mM Ca^{2+} , can cause significant aggregation of lipidic structures at the interfaces, leading to a situation where a well defined single SLB cannot be obtained. At high (20 mM) Ca^{2+} concentration not even significant adsorption could be achieved for most of the investigated systems, demonstrating that in order to use Ca^{2+} to facilitate SLB formation by negatively charged liposome fusion Ca^{2+} has to be tuned in a narrow range between ~0–5 mM.

VI. CONCLUSIONS

We have shown that the formation of planar supported lipid bilayers can be achieved using a Ca^{2+} -containing buffer for a wider range of lipid compositions than previously demonstrated. Especially, TiO_2 is a suitable substrate for this strategy. On TiO_2 the main mechanism seems to be the electrostatic interaction between Ca^{2+} accumulated at the solid interface interacting with anionic lipid head groups. In particular, we have found proper conditions for forming SLB for three lipid compositions mimicking *E. coli* lipid membranes, including *E. coli* total lipid extract on typical biosensor coatings. These model systems can be of great benefit for studying the interaction of antibiotic compounds thought to act on bacterial membranes using membrane-modified biosensor supports.

Complete bacterial mimic SLB could not be formed on ITO, although it was shown that, for other lipid mixtures used as controls, SLB formation on ITO can easily occur and, especially in the presence of calcium with anionic liposomes, lead to fast rupture of liposomes on the surface and a tightly bound SLB.

In the act of proving that *E. Coli* total lipid extract can

form SLB, it was demonstrated how measurements with complementary techniques are imperative to correctly interpret data for membrane structures undergoing conformational changes and assuming dynamic 3D structures. The hypothesis fitting the combined results of QCM-D, OWLS, and FRAP was that of an undulating SLB, which by QCM-D alone traditionally would be classified as a partial SLB, by OWLS showing an unusually high lipid mass, and by FRAP an unusual and slow fluorescence recovery. The high complexity of the *E. coli* total lipid extract mixture and potential surface-induced lipid phase segregation was the likely reason for formation of the —with time—increasingly nonplanar SLB. This has implications for future creation of other SLB with complex composition, where thus not only segregation of lipids between the two leaflets but also conformational changes induced by transversal or lateral lipid phase segregation could be observed.

ACKNOWLEDGMENTS

The authors acknowledge the Paul Scherrer Institute for help with surface coating. ETH Zurich, Competence Center for Materials Science and Technology (CCMX), Switzerland and A*STAR, Singapore are acknowledged for financial support.

- ¹E. T. Castellana and P. S. Cremer, *Surf. Sci. Rep.* **61**, 429 (2006).
- ²R. Naumann *et al.*, *Langmuir* **19**, 5435 (2003).
- ³E. Reimhult, Z. Zach, F. Hook, and B. Kasemo, *Langmuir* **22**, 3313 (2006).
- ⁴J. Voros, J. J. Ramsden, G. Csucs, I. Szendro, S. M. De Paul, M. Textor, and N. D. Spencer, *Biomaterials* **23**, 3699 (2002).
- ⁵R. Horvath, G. Fricovszky, and E. Papp, *Biosens. Bioelectron.* **18**, 415 (2003).
- ⁶C. A. Keller and B. Kasemo, *Biophys. J.* **75**, 1397 (1998).
- ⁷R. P. Richter, R. Berat, and A. R. Brisson, *Langmuir* **22**, 3497 (2006).
- ⁸H. M. McConnell, T. H. Watts, R. M. Weis, and A. A. Brian, *Biochim. Biophys. Acta* **864**, 95 (1986).
- ⁹H. Schonherr, J. M. Johnson, P. Lenz, C. W. Frank, and S. G. Boxer, *Langmuir* **20**, 11600 (2004).
- ¹⁰P. Lenz, C. M. Ajo-Franklin, and S. G. Boxer, *Langmuir* **20**, 11092 (2004).
- ¹¹J. M. Johnson, T. Ha, S. Chu, and S. G. Boxer, *Biophys. J.* **83**, 3371 (2002).
- ¹²R. P. Richter and A. R. Brisson, *Biophys. J.* **88**, 3422 (2005).
- ¹³R. P. Richter, N. Maury, and A. R. Brisson, *Langmuir* **21**, 299 (2005).
- ¹⁴R. Richter, A. Mukhopadhyay, and A. Brisson, *Biophys. J.* **85**, 3035 (2003).
- ¹⁵R. P. Richter and A. Brisson, *Langmuir* **19**, 1632 (2003).
- ¹⁶I. Reviakine, A. Simon, and A. Brisson, *Langmuir* **16**, 1473 (2000).
- ¹⁷I. Reviakine and A. Brisson, *Langmuir* **16**, 1806 (2000).
- ¹⁸B. Seantier, C. Breffa, O. Felix, and G. Decher, *J. Phys. Chem. B* **109**, 21755 (2005).
- ¹⁹S. Boudard, B. Seantier, C. Breffa, G. Decher, and O. Felix, *Thin Solid Films* **495**, 246 (2006).
- ²⁰B. Seantier, C. Breffa, O. Felix, and G. Decher, *Nano Lett.* **4**, 5 (2004).
- ²¹K. Dimitrievski, E. Reimhult, B. Kasemo, and V. P. Zhdanov, *Colloids Surf., B* **39**, 77 (2004).
- ²²E. Reimhult, F. Hook, and B. Kasemo, *Phys. Rev. E* **66**, 051905 (2002).
- ²³E. Reimhult, F. Hook, and B. Kasemo, *J. Chem. Phys.* **117**, 7401 (2002).
- ²⁴E. Reimhult, F. Hook, and B. Kasemo, *Langmuir* **19**, 1681 (2003).
- ²⁵F. F. Rossetti, M. Textor, and I. Reviakine, *Langmuir* **22**, 3467 (2006).
- ²⁶F. F. Rossetti, M. Bally, R. Michel, M. Textor, and I. Reviakine, *Langmuir* **21**, 6443 (2005).
- ²⁷L. J. C. Jeuken, S. D. Connell, M. Nurnabi, J. O'Reilly, P. J. F. Henderson, S. D. Evans, and R. J. Bushby, *Langmuir* **21**, 1481 (2005).
- ²⁸P. Nollert, H. Kiefer, and F. Jahnig, *Biophys. J.* **69**, 1447 (1995).
- ²⁹E. Kalb, S. Frey, and L. K. Tamm, *Biochim. Biophys. Acta* **1103**, 307 (1992).
- ³⁰H. Barman, M. Walch, S. Latinovic-Golic, C. Dumrese, M. Dolder, P. Groscurth, and U. Ziegler, *J. Membr. Biol.* **212**, 29 (2006).
- ³¹S. Garcia-Manyes, G. Oncins, and F. Sanz, *Biophys. J.* **89**, 1812 (2005).
- ³²S. Faiss, E. Luthgens, and A. Janshoff, *Eur. Biophys. J.* **33**, 555 (2004).
- ³³N. Papo and Y. Shai, *Biochemistry* **43**, 6393 (2004).
- ³⁴M. L. Wagner and L. K. Tamm, *Biophys. J.* **79**, 1400 (2000).
- ³⁵C. Steinem, A. Janshoff, F. Hohn, M. Sieber, and H. J. Galla, *Chem. Phys. Lipids* **89**, 141 (1997).
- ³⁶M. Stelzle, G. Weissmuller, and E. Sackmann, *J. Phys. Chem.* **97**, 2974 (1993).
- ³⁷Z. Salamon, G. Lindblom, L. Rilfors, K. Linde, and G. Tollin, *Biophys. J.* **78**, 1400 (2000).
- ³⁸Z. Salamon, G. Lindblom, and G. Tollin, *Biophys. J.* **84**, 1796 (2003).
- ³⁹J. H. Tong and T. J. McIntosh, *Biophys. J.* **86**, 3759 (2004).
- ⁴⁰L. J. C. Jeuken, S. D. Connell, P. J. F. Henderson, R. B. Gennis, S. D. Evans, and R. J. Bushby, *J. Am. Chem. Soc.* **128**, 1711 (2006).
- ⁴¹T. Ganz, *Nat. Rev. Immunol.* **3**, 710 (2003).
- ⁴²O. Toke, *Biopolymers* **80**, 717 (2005).
- ⁴³M. Rodahl and B. Kasemo, *Rev. Sci. Instrum.* **67**, 3238 (1996).
- ⁴⁴G. Sauerbrey, *Z. Phys.* **155**, 206 (1959).
- ⁴⁵J. A. de Feijter, J. Benjamins, and F. A. Veer, *Biopolymers* **17**, 1759 (1978).
- ⁴⁶G. Csucs and J. J. Ramsden, *Biochim. Biophys. Acta* **1369**, 61 (1998).
- ⁴⁷C. Larsson, M. Rodahl, and F. Höök, *Anal. Chem.* **75**, 5080 (2003).
- ⁴⁸Z. Salamon and G. Tollin, *Biophys. J.* **80**, 1557 (2001).
- ⁴⁹A. Lopez, L. Dupou, A. Altibelli, J. Trotard, and J. F. Tocanne, *Biophys. J.* **53**, 963 (1988).
- ⁵⁰D. Axelrod, D. E. Koppel, J. Schlessinger, E. Elson, and W. W. Webb, *Biophys. J.* **16**, 1055 (1976).
- ⁵¹E. Reimhult, C. Larsson, B. Kasemo, and F. Hook, *Anal. Chem.* **76**, 7211 (2004).
- ⁵²C. A. Keller, K. Glasmästar, V. P. Zhdanov, and B. Kasemo, *Phys. Rev. Lett.* **84**, 5443 (2000).
- ⁵³J. T. Groves, N. Ulman, and S. G. Boxer, *Science* **275**, 651 (1997).
- ⁵⁴K. Glasmästar, C. Larsson, F. Höök, and B. Kasemo, *J. Colloid Interface Sci.* **246**, 40 (2002).
- ⁵⁵K. J. Seu, E. R. Lamberson, and J. S. Hovis, *J. Phys. Chem. B* **111**, 6289 (2007).
- ⁵⁶L. R. Cambrea and J. S. Hovis, *Biophys. J.* **92**, 3587 (2007).
- ⁵⁷L. S. Jung, C. T. Campbell, T. M. Chinowsky, M. N. Mar, and S. S. Yee, *Langmuir* **14**, 5636 (1998).
- ⁵⁸J. M. Crane, V. Kiessling, and L. K. Tamm, *Langmuir* **21**, 1377 (2005).
- ⁵⁹M. Kasbauer, M. Junglas, and T. M. Bayerl, *Biophys. J.* **76**, 2600 (1999).
- ⁶⁰M. Kosmulski, J. Gustafsson, and J. B. Rosenholm, *Colloid Polym. Sci.* **277**, 550 (1999).
- ⁶¹M. Kosmulski, J. Hartikainen, E. Maczka, W. Janusz, and J. B. Rosenholm, *Anal. Chem.* **74**, 253 (2002).
- ⁶²E. McCafferty, J. P. Wightman, and T. F. Cromer, *J. Electrochem. Soc.* **146**, 2849 (1999).
- ⁶³O. Sneh and S. M. George, *J. Phys. Chem.* **99**, 4639 (1995).
- ⁶⁴M. E. Haque, T. J. McIntosh, and B. R. Lentz, *Biochemistry* **40**, 4340 (2001).
- ⁶⁵I. Reviakine, F. F. Rossetti, A. N. Morozov, and M. Textor, *J. Chem. Phys.* **122**, 204711 (2005).
- ⁶⁶U. Seifert, *Adv. Phys.* **46**, 13 (1997).
- ⁶⁷U. Seifert and R. Lipowsky, *Phys. Rev. A* **42**, 4768 (1990).
- ⁶⁸V. P. Zhdanov, C. A. Keller, K. Glasmästar, and B. Kasemo, *J. Chem. Phys.* **112**, 900 (2000).
- ⁶⁹T. M. Bayerl and M. Bloom, *Biophys. J.* **58**, 357 (1990).
- ⁷⁰H. Gao, G. A. Luo, F. B. Jun, A. L. Ottova, and H. T. Tien, *J. Electroanal. Chem.* **496**, 158 (2001).
- ⁷¹H. Hillebrandt, M. Tanaka, and E. Sackmann, *J. Phys. Chem. B* **106**, 477 (2002).
- ⁷²H. Hillebrandt, G. Wiegand, M. Tanaka, and E. Sackmann, *Langmuir* **15**, 8451 (1999).
- ⁷³S. Gritsch, P. Nollert, F. Jahnig, and E. Sackmann, *Langmuir* **14**, 3118 (1998).
- ⁷⁴G. Wiegand, N. Arribas-Layton, H. Hillebrandt, E. Sackmann, and P. Wagner, *J. Phys. Chem. B* **106**, 4245 (2002).
- ⁷⁵B. R. Lentz and J. K. Lee, *Mol. Membr. Biol.* **16**, 279 (1999).